



Filippi, Gianluca and Krpelik, Daniel and Korondi, Peter Zeno and Vasile, Massimiliano and Marchi, Mariapia and Poloni, Carlo (2018) Space systems resilience engineering and global system reliability optimisation under imprecision and epistemic uncertainty. In: 69th International Astronautical Congress, 2018-10-01 - 2018-10-05. ,

This version is available at <https://strathprints.strath.ac.uk/65986/>

Strathprints is designed to allow users to access the research output of the University of Strathclyde. Unless otherwise explicitly stated on the manuscript, Copyright © and Moral Rights for the papers on this site are retained by the individual authors and/or other copyright owners. Please check the manuscript for details of any other licences that may have been applied. You may not engage in further distribution of the material for any profitmaking activities or any commercial gain. You may freely distribute both the url (<https://strathprints.strath.ac.uk/>) and the content of this paper for research or private study, educational, or not-for-profit purposes without prior permission or charge.

Any correspondence concerning this service should be sent to the Strathprints administrator: strathprints@strath.ac.uk

IAC-18-D1.4B.11x46693

Space Systems Resilience Engineering and Global System Reliability Optimisation Under Imprecision and Epistemic Uncertainty

Gianluca Filippi^{a,*}, Daniel Krpelik^{b,c}, Peter Zeno Korondi^{d,e}, Massimiliano Vasile^a,
Mariapia Marchi^d, Carlo Poloni^{d,e}

^a*Department of Mechanical & Aerospace Engineering, University of Strathclyde, James Weir Building, 75 Montrose Street, Glasgow, United Kingdom G11XJ, g.filippi@strath.ac.uk*

^b*Department of Mathematical Sciences, Durham University, Lower Mountjoy, Stockton Rd, Durham, DH1 3LE, United Kingdom, daniel.krpelik@durham.ac.uk*

^c*Department of Applied Mathematics, VŠB-Technical University of Ostrava, 17. listopadu 15/2172, 708 33 Ostrava-Poruba, Czech Republic*

^d*Numerical Methods Group, ESTECO S.p.A, Building B, 99 Padriciano, Area Science Park, Trieste, Italy 34149, korondi@esteco.com*

^e*Department of Engineering and Architecture, University of Trieste, Piazzale Europa 1, Trieste, Italy 34127*

*Corresponding Author

Abstract

The paper introduces the concept of design for resilience in the context of space systems engineering and proposes a method to account for imprecision and epistemic uncertainty. Resilience can be seen as the ability of a system to adjust its functioning prior to, during, or following changes and disturbances, so that it can sustain required operations under both expected and unexpected conditions. Mathematically speaking this translates into the attribute of a dynamical system (or time dependent system) to be simultaneously robust and reliable. However, the quantification of robustness and reliability in the early stage of the design of a space systems is generally affected by uncertainty that is epistemic in nature. As the design evolves from Phase A down to phase E, the level of epistemic uncertainty is expected to decrease but still a level of variability can exist in the expected operational conditions and system requirements. The paper proposes a representation of a complex space system using the so called Evidence Network Models (ENM): a non-directed (unlike Bayesian network models) network of interconnected nodes where each node represents a subsystem with associated epistemic uncertainty on system performance and failure probability. Once the reliability and uncertainty on the performance of the spacecraft are quantified, a design optimisation process is applied to improve resilience and performance. The method is finally applied to an example of preliminary design of a small satellite in Low Earth Orbit (LEO). The spacecraft is divided in 5 subsystems, AOCS, TTC, OBDH, Power and Payload. The payload is a simple camera acquiring images at scheduled times. The assumption is that each component has multiple functionalities and both the performance of the component and the reliability associated to each functionality are affected by a level of imprecision. The overall performance indicator is the sum of the performance indicators of all the components.

Keywords: Epistemic uncertainty, Resilient satellite, Complex systems, Evidence Theory

Nomenclature	\mathbf{u}_{ij}	Coupled uncertain epistemic variables
\mathbf{d}		Deterministic design variables
	θ	Focal elements
\mathbf{u}_i		Uncoupled uncertain epistemic variables
	C	Generic constraint function

F Generic objective function
 t Continuous time variable

Acronyms

AOCS Attitude and Orbit Control Subsystem

bpa basic probability assignment

DST Dempster Shafer Theory

ENM Evidence Network Model

FE Focal Element

LEO Low Earth Orbit

MPAIDEA Multi-Population Adaptive Inflationary Differential Evolution Algorithm

OBDH On-board Data Handling

TTC Telemetry, Tracking and Command

1. Introduction

The adverse environment of space makes risk reduction a key objective in satellite design. The maintenance of an on-orbit satellite is very limited or even impossible. Therefore, risk reduction is achieved by designing the satellite for robustness and reliability considering the entire lifetime. Robustness is here considered by evaluating the worst case scenario; this approach was introduced in [1, 2]. A generalisation is then provided by [3] that introduces the constraints satisfaction.

Traditionally, safety margins and redundancy are employed to reach reliable performance. This traditional method lacks of estimating the uncertainties properly. Uncertainty overestimation can lead to significant increase of the expenses. Contrarily, underestimation of the uncertainties can lead to unrecoverable failure of the entire system. This motivated the community to develop various taxonomy and uncertainty quantification methods for engineering design. In this paper, we divide the uncertainty into two categories: *aleatory uncertainty* and *epistemic uncertainty*.

Aleatory uncertainty is a natural randomness which cannot be reduced. The precise probability theory provides a sound mathematical tool to describe its characteristics. Epistemic uncertainty is due to the lack of information or incomplete data. This type of uncertainty is reducible by acquiring

more knowledge on the problem. Epistemic uncertainty can be modelled by Evidence Theory which also known as Dempster-Shafer theory (DST) [4, 5, 6].

A recent technique for engineering system design based on the Evidence Theory was introduced in [7]. The technique is called Evidence Network Model (ENM) and the method was extended in [8] to make ENM computationally more efficient.

This work extends the ENM and [9] - that introduces time-dependencies reliability in the system model - to enable its usage for resilient system design.

In this work, a small satellite in Low Earth Orbit (LEO) is designed with the proposed method. The satellite is designed to take pictures of the Earth and reliably operate during its entire lifetime. The space system is composed of 5 subsystems. The reliability and performance of each subsystem is subjected to epistemic uncertainties.

2. Evidence Network Models

DST combines different and conflicting sources of information and assigns to each possible event a probability mass called *basic probability assignment* (bpa).

A generic engineering system is affected by both design parameters $d \in D$ and uncertain parameters $u \in U$. Then DST assigns to each u one or more sets with a corresponding bpa. The system can be represented as a network of nodes that share information (see Figure 1 for example) where each node is a subsystem and information is shared through the links between subsystems. The generic objective function can then be defined as:

$$F(\mathbf{d}, \mathbf{u}) = \sum_{i=1}^N g_i(\mathbf{d}, \mathbf{u}_i, \mathbf{h}_i(\mathbf{d}, \mathbf{u}_i, \mathbf{u}_{ij})), \quad (1)$$

where N is the number of subsystems involved, $\mathbf{h}_i(\mathbf{d}, \mathbf{u}_i, \mathbf{u}_{ij})$ is the vector of scalar functions $h_{ij}(\mathbf{d}, \mathbf{u}_i, \mathbf{u}_{ij})$ where $j \in J_i$ and J_i is the set of indexes of nodes connected to the i -th node; \mathbf{u}_i are the uncertain variables of subsystem i not shared with any other subsystem and \mathbf{u}_{ij} are the uncertain variables shared among subsystems i and j .

Given a design, or decision, value $\tilde{\mathbf{d}} \in D$, we will call *worst case scenario* the vector $\underline{\mathbf{u}}$ that corresponds to the maximum of F over the space U :

$$\underline{\mathbf{u}} = \underset{\mathbf{u} \in U}{\operatorname{argmax}} F(\tilde{\mathbf{d}}, \mathbf{u}). \quad (2)$$

Likewise we can call *best case scenario* the quantity:

$$\bar{\mathbf{u}} = \underset{\mathbf{u} \in U}{\operatorname{argmin}} F(\tilde{\mathbf{d}}, \mathbf{u}). \quad (3)$$

We can now define an event in the space U , or a proposition on the value of F , as the set A such that:

$$A = \{\mathbf{u} \in U \mid F(\mathbf{d}, \mathbf{u}) \leq \nu\}. \quad (4)$$

We can finally define two quantities associated to the belief in the occurrence of the event A :

$$Bel(A) = \sum_{\theta \subset A, \theta \in U} bpa(\theta), \quad (5)$$

$$Pl(A) = \sum_{\theta \cap A \neq \emptyset, \theta \in U} bpa(\theta), \quad (6)$$

where $bpa(\theta)$ is the basic probability assignment associated to the FE θ . More details about the theory can be found in [6]. Accordingly, with DST the computational cost of exact Belief (Bel) - (Plausibility (Pl) respectively) - curve is exponential with the system dimension because a maximisation (minimisation respectively) for each FE θ is needed, where the FEs are constructed from the cross product of all the intervals of all the parameters $u \in U$.

3. Decomposition Algorithm

The computational issue expressed at the end of the previous section is motivated the use of the Decomposition approach based on the ENM. The algorithm aims at decoupling the subsystems over the uncertain variables in order to optimise only over a small subset of the FEs. The approach is explained by Algorithm 1 for the reconstruction of the Bel curve and it can be summarised as follow:

1. Solution of the optimal worst case scenario problems (lines 12, 13 and 14).
2. Maximisation over the coupled variables and computation of m_c partial $Bel_c(A)$ curves.
3. Maximisation over the uncoupled variables.
4. Reconstruction of the approximation $\widetilde{Bel}(A)$.

The Plausibility curve can be calculated analogously by replacing the steps of uncertainty maximisation with uncertainty minimisation.

The effectiveness of the Decomposition algorithm is well presented by the cost reduction. As explained in the previous section, the total number of FEs to explore for a problem with m uncertain variables, each defined over N_k intervals, is:

$$N_{FE} = \prod_{k=1}^m N_k. \quad (7)$$

In terms of coupled and uncoupled uncertain vectors we can write:

$$N_{FE} = \left(\prod_{i=1}^{m_u} \prod_{k=1}^{p_i^u} N_{i,k}^u \right) \left(\prod_{i=1}^{m_c} \prod_{k=1}^{p_i^c} N_{i,k}^c \right), \quad (8)$$

where p_i^u and p_i^c are the number of components of the i^{th} uncoupled and coupled vector, respectively, and $N_{i,k}^u$ and $N_{i,k}^c$ are the numbers of intervals of the k^{th} components of the i^{th} uncoupled and coupled vector respectively. The total number of FE, over which we have to optimise in the decomposition, is instead:

$$N_{FE}^{Dec} = N_s \sum_{i=1}^{m_u} N_{FE,i}^u + \sum_{i=1}^{m_c} N_{FE,i}^c, \quad (9)$$

considering the vector of uncertainties ordered as:

$$\mathbf{u} = \underbrace{[\mathbf{u}_1, \dots, \mathbf{u}_{m_u}]}_{\text{uncoupled}}, \underbrace{[\mathbf{u}_1, \dots, \mathbf{u}_{m_c}]}_{\text{coupled}}, \quad (10)$$

where and N_s is the number of samples in the partial belief curves, $N_{FE,i}^c = \prod_{k=1}^{p_i^c} N_{i,k}^c$ and $N_{FE,i}^u = \prod_{k=1}^{p_i^u} N_{i,k}^u$. This means that the computational complexity to calculate the maxima of the function F within the FEs remains exponential for each individual uncoupled or coupled vector but it is polynomial with the number of subsystems.

A comprehensive presentation of the Decomposition approach is in [8].

4. Constrained Minmax

The approach to the design of complex systems under uncertainty proposed in this paper requires the solution of one or more constrained minmax optimisation problems:

$$\begin{aligned} \min_{\mathbf{d} \in D} \max_{\mathbf{u} \in U} F(\mathbf{d}, \mathbf{u}) \\ \text{s.t.} \\ C(\mathbf{d}, \mathbf{u}) \leq 0. \end{aligned} \quad (11)$$

The solution to this class of problem is here approached with a constrained variant of Multi-Population Adaptive Inflationary Differential Evolution Algorithm (MPAIDEA), an adaptive version of Inflationary Differential Evolution [2]. This section describes only the strategy to handle constraints in the minmax version of MPAIDEA. More details on the approach to the solution of unconstrained minmax problems with Inflationary Differential Evolution can be found in [1].

Algorithm 1 Decomposition

```

1: Initialise
2: Uncoupled vectors  $\mathbf{u}_u = [\mathbf{u}_1, \mathbf{u}_2, \dots, \mathbf{u}_i, \dots, \mathbf{u}_{m_u}]$ 
3: Coupled vectors  $\mathbf{u}_c = [\mathbf{u}_{12}, \mathbf{u}_{13}, \dots, \mathbf{u}_{ij}, \dots, \mathbf{u}_{m_c}]$ 
4: for a given design  $\tilde{\mathbf{d}}$  do
5:   Compute  $(\tilde{\mathbf{d}}, \underline{\mathbf{u}}_u, \underline{\mathbf{u}}_c) = \operatorname{argmax} F(\tilde{\mathbf{d}}, \underline{\mathbf{u}}_u, \underline{\mathbf{u}}_c)$ 
6:   for all  $\mathbf{u}_{ij} \in \mathbf{u}_c$  do
7:     for all FE  $\theta_{k,ij} \subseteq \Theta_{ij}$  do
8:        $\hat{F}_{k,ij} = \max_{\mathbf{u}_{ij} \in \theta_{k,ij}} F(\tilde{\mathbf{d}}, \underline{\mathbf{u}}_u, \mathbf{u}_{ij})$ 
9:        $\hat{\mathbf{u}}_{k,ij} = \operatorname{argmax}_{\mathbf{u}_{ij} \in \theta_{k,ij}} F$ 
10:      Evaluate  $bpa(\theta_{k,ij})$ 
11:      Evaluate partial Belief curve  $Bel(F(\mathbf{u}_{ij}) \leq \nu)$ 
12:    end for
13:    for number of samples do
14:      Evaluate  $\Delta Bel^q, \hat{\mathbf{u}}_{k,ij}$  and  $\hat{F}_{k,ij}$ 
15:    end for
16:  end for
17:  for all the combinations of samples do
18:    for all  $\mathbf{u}_i \in \mathbf{u}_u$  do
19:      for all FE  $\theta_{k,i} \subseteq \Theta_i$  do
20:         $F_{max,k,i} = \max_{\mathbf{u}_i \in \theta_{k,i}} F(\tilde{\mathbf{d}}, \hat{\mathbf{u}}_c, \mathbf{u}_i)$ 
21:        Evaluate  $bpa(\theta_{k,i})$ 
22:      end for
23:    end for
24:    for all the combinations of FE
25:     $\theta_t \in \Theta_1 \times \Theta_2 \times \dots \times \Theta_{m_u}$  do
26:      Evaluate  $F_{max,k} \leq \nu$ 
27:      Evaluate  $bpa_k$ 
28:    end for
29:    Evaluate the Belief for this sample by constructing
    collection  $\Gamma_\nu$ 
30:  end for
31:  Add up all belief values for all samples
32: end for

```

The minmax algorithm proposed in this paper iteratively solves a bi-level optimisation, first minimising over the design vector \mathbf{d} (outer loop) and then maximising over the uncertainty vector \mathbf{u} (inner loop). The inner loop provides solutions that satisfy the constraint; while the outer loop maintains the constraint satisfaction while minimising the cost function F . The constraint handling procedure, summarised in Algorithm 2, implements the following steps:

- Initialisation of a population of \mathbf{d} and \mathbf{u} vectors;
- While the number function evaluations is lower than N_{feval}^{max} function evaluations, do the following
 - [Outer Loop] Constrained minimisation of the objective function over the design space, evalu-

ating the cost function F over all the uncertainty vectors stored in an archive $A = A_u \cup A_c$:

$$\begin{aligned} & \min_{\mathbf{d} \in D \wedge \mathbf{u} \in A} F(\mathbf{d}, \mathbf{u}) \\ & s.t. \\ & \max_{\mathbf{u} \in A} C(\mathbf{d}, \mathbf{u}) \leq 0 \end{aligned} \quad (12)$$

- [Inner Loop] Constrained maximisation of the cost function F over the uncertain parameters \mathbf{u} and parallel maximisation of the constraint violation over the uncertainty space:

$$\begin{aligned} & \max_{\mathbf{u} \in U} F(\mathbf{d}_{min}, \mathbf{u}) \\ & s.t. \\ & C(\mathbf{d}_{min}, \mathbf{u}) \leq 0 \end{aligned} \quad (13)$$

$$\max_{\mathbf{u} \in U} C(\mathbf{d}_{min}, \mathbf{u}) \quad (14)$$

$\mathbf{u}_{a,F} = \operatorname{argmax}_{\mathbf{u} \in U} F(\mathbf{d}_{min}, \mathbf{u})$ is added to the archive A_u and $\mathbf{u}_{a,C} = \operatorname{argmax}_{\mathbf{u} \in U} C(\mathbf{d}_{min}, \mathbf{u})$ is added to A_c if $\max_{\mathbf{u} \in U} C(\mathbf{d}, \mathbf{u}) > 0$. This approach pushes the optimiser to find design configurations that are feasible for all values of the uncertain variables. If a feasible solution cannot be found, the constraints are relaxed (line 24 in Algorithm 2) in the Inner Loop by computing a new constraint $C^* = C + \epsilon$ with ϵ the minimum constraint violation over U .

In the multi-objective optimisation:

- Cross-check of the final solutions and choice of the best design;
- Final maximisation over U .

5. The performance function

The test case function used to validate the proposed approach describes the operations of a cube-sat in Low Earth Orbit (LEO). The problem is affected by epistemic uncertainty modelled with the use of DST [4, 5, 6] and in particular the ENM presented in [7, 8] is used to evaluate the associated Belief and Plausibility curves. The robustness of the solution is guaranteed by the minmax algorithm described in [1, 2, 3] and finally, considering three possible operational states, the resilience of the system during its mission is optimised.

The problem is to minimise the mass of the satellite and maximise the amount of data sent back to the ground station. These performance indices depend on 16 design parameters

Table 1: Design parameters.

SYSTEMS	\mathbf{d}	LB	UB
PAYLOAD	BD	1	5
	P_{day} (W)	2.5	4
	P_{night} (W)	0	9.75
	image size (pixel)	307200	5038848
	FR_{max} (sec^{-1})	6.6	26.6
OBDH	type	1	6
AOCS	t_{slew} (sec)	30	90
	ϕ_{slew} (deg)	10	60
TTC	f (GHz)	7	10
	modulation	0	1
	amplifier	TWP	SSP
POWER	V_{bus} (V)	3	5
	V_{drop} (%)	1	5
	configuration	DET	MPPT
	η_{cell}	0.15	0.3
	E_{cell} (Wh)	135	145

Table 2: Uncertain parameters.

SYSTEMS	\mathbf{u}	interval 1	interval 2
PAYLOAD	H (km)	[600 800]	[800 1000]
	ϵ (deg)	[0 5]	[5 10]
	δI (%)	[0 5]	[5 10]
OBDH	δP (%)	[0 10]	[10 20]
	δM (%)	[0 10]	[10 20]
AOCS	l (m)	[0.005 0.01]	[0.01 0.02]
	A (m^2)	[0.034 0.0885]	[0.0885 0.15]
	q	[0.5 0.6]	[0.6 0.7]
	m ($mA \cdot m^2$)	[0.5 1]	[1 1.5]
	C_D	[2 2.2]	[2.2 2.5]
	δI (%)	[-10 5]	[5 10]
TTC	η_{ant}	[0.6 0.8]	[0.8 0.9]
	G_t (dB)	[1 3]	3 5
	L_t (dB)	[0.1 0.5]	[0.5 1]
	L_{other} (dB)	[0.5 1.5]	[1.5 2.0]
	M_{rfdn} (kg)	[0.1 0.3]	[0.2 0.5]
	POWER	D_{cell}	[0.025 0.0275]
η_a		[0.8 0.85]	[0.85 0.9]
ρ_{sa} (kg/m^2)		[3.5 3.6]	[3.6 4]
δP (%)		[0 10]	[10 20]
T_{max} (C)		[0 10]	[10 15]

Algorithm 2 Constrained minmax

```

1: Initialise  $\bar{\mathbf{d}}$  at random and run  $\mathbf{u}_a = \operatorname{argmax} F(\bar{\mathbf{d}}, \mathbf{u})$ 
   s.t.  $C(\mathbf{d}_{min}, \mathbf{u}) \leq 0$ 
2:
3:  $A_u = A_u \cup \{\mathbf{u}_a\}$ ;  $A_c = \emptyset$ ;  $A_d = \emptyset$ 
4: while  $N_{fval} < N_{fval}^{max}$  do
5:   Outer loop:
6:
7:    $\mathbf{d}_{min} = \operatorname{argmin}_{\mathbf{d} \in D} \{\max_{\mathbf{u} \in A_u \cup A_c} F(\mathbf{d}, \mathbf{u})\}$  s.t.
8:  $\max_{\mathbf{u} \in A_u \cup A_c} C(\mathbf{d}, \mathbf{u}) \leq 0$ 
9:
10:   $A_d = A_d \cup \{\mathbf{d}_{min}\}$ 
11:  Inner loop:
12:
13:   $\mathbf{u}_{a,F} = \operatorname{argmax}_{\mathbf{u} \in U} F(\mathbf{d}_{min}, \mathbf{u})$  s.t.  $C(\mathbf{d}_{min}, \mathbf{u}) \leq 0$ 
14:
15:   $\mathbf{u}_{a,C} = \operatorname{argmax}_{\mathbf{u} \in U} C(\mathbf{d}_{min}, \mathbf{u})$ 
16:
17:   $A_u = A_u \cup \{\mathbf{u}_{a,F}\}$ 
18:  if  $N_{fval} < N_{relaxation}^{\vee}$ 
19:   $\exists \mathbf{d} \in A_d$  t.c.  $\max_{\mathbf{u} \in U} C(\mathbf{d}, \mathbf{u}) \leq 0$  then
20:    if  $\max_{\mathbf{u} \in U} C(\mathbf{d}_{min}, \mathbf{u}) > 0$  then
21:       $A_c = A_c \cup \{\mathbf{u}_{a,C}\}$ 
22:    end if
23:  else
24:    update  $\epsilon$ 
25:     $A_c = \{A_c \setminus \mathbf{u}_{a,C} \mid C(\mathbf{d}_{min}, \mathbf{u}) \leq \epsilon\}$ 
26:    if  $\max_{\mathbf{u} \in U} C(\mathbf{d}_{min}, \mathbf{u}) > \epsilon$  then
27:       $A_c = A_c \cup \{\mathbf{u}_{a,C}\}$ 
28:    end if
29:  end if
30: end while

```

(listed in Table 1) and 21 uncertain parameters (listed in Table 2) where the uncertain vector can be decomposed by the following Equation 10:

$$\mathbf{u}_{uncoupled} = [\mathbf{u}_{OBDH}, \mathbf{u}_{TTC}, \mathbf{u}_{POWER}, \mathbf{u}_{AOCS}]$$

and

$$\mathbf{u}_{coupled} = [\mathbf{u}_{AOCS-POWER}, \mathbf{u}_{AOCS-PL}, \mathbf{u}_{TTC-POWER}, \mathbf{u}_{OBDH-POWER}]$$

and $\dim(\mathbf{u}_{OBDH}) = 1$, $\dim(\mathbf{u}_{TTC}) = 2$, $\dim(\mathbf{u}_{POWER}) = 5$, $\dim(\mathbf{u}_{AOCS}) = 2$, $\dim(\mathbf{u}_{AOCS-POWER}) = 4$, $\dim(\mathbf{u}_{AOCS-PL}) = 3$, $\dim(\mathbf{u}_{TTC-POWER}) = 3$, $\dim(\mathbf{u}_{OBDH-POWER}) = 1$. In our scenario, the performance of the satellite is measured by the amount of information transmitted back to the ground station, or total Data Volume, V , and the overall mass of the system, M .

For a given value of the design and uncertain parameters, one can calculate the amount of information transmitted during each orbit, V_i . The total amount of transmitted information is the sum of the data volume over all completed orbits within the predefined mission time, $T_{Mission}$. The total data volume is a function of the possible failure states of the satellite. The type of failure influences how the satellite operates and, consequently, how much information is transmitted. The transition between states of the satellite is described by a (precise) stochastic process. Thus the value of the data volume is affected by the uncertain parameters \mathbf{u} but also by the sequence of state transitions. Hence, in the following, we use as performance indicator the expected cumulative value of the data volume:

$$f_{DV}(\mathbf{d}, \mathbf{u}, t) = \mathbb{E} \left\{ \sum_{i=1}^{N_o} V_i^c(X, \mathbf{d}, \mathbf{u}, t) \right\}, \quad (15)$$

where V_i^c denotes the volume of (compressed) data (see Equation 30) transmitted during the i -th orbit, X is a random variable representing the whole evolution of state of the system, N_o is the total amount of orbits during the planned mission of the satellite and the evaluation of the expected value is explained in Sections 6 and 6.1.

In order to account for both objectives M and f_{DV} we consider the following two problems:

$$\min_{\mathbf{d} \in \mathcal{D}} \max_{\mathbf{u} \in \mathcal{U}} \frac{M_{TOT}(\mathbf{d}, \mathbf{u}, t)}{f_{DV}(\mathbf{d}, \mathbf{u}, t)} \quad (16)$$

$$\min_{\mathbf{d} \in \mathcal{D}} \left(\max_{\mathbf{u} \in \mathcal{U}} M_{TOT}(\mathbf{d}, \mathbf{u}, t), \max_{\mathbf{u} \in \mathcal{U}} f_{DV}(\mathbf{d}, \mathbf{u}, t) \right) \quad (17)$$

Problem (16) uses a single scalarised objective function while Problem (17) solves a full multi-objective problem with a vector objective function.

5.1 Cube-sat system

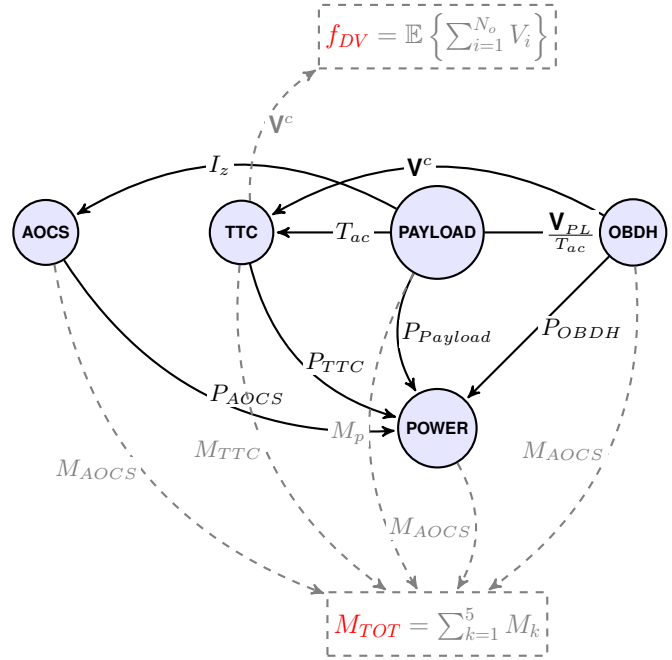


Fig. 1: Representation of the cube-sat as a complex system. The two quantities of interest are the mass of the cubesat M_{TOT} and the total amount of data transmitted to the ground station f_{DV} ; M_{TOT} is the sum of the mass of the 5 subsystems and f_{DV} is the quantities of data sent by the TTC after the compression in OBBDH.

The considered cube-sat is a complex system composed of 5 subsystems interconnected as in Figure 1.

5.2 Payload

The payload is a camera that takes images of the atmosphere and send them to the OBBDH for the compression. Images are taken only during light-time; for the generic i -th orbit is $T_{light}^i = T_{orbit} - T_{eclipse}$ where the eclipse time is approximated as function of the altitude only:

$$T_{eclipse}(H) = \frac{EAD \cdot T_{orbit}}{360^\circ} \quad (18)$$

with the Earth Angular Diameter $EAD = 2 \arcsin\left(\frac{R_E}{H+R_E}\right)$ where R_E is the Earth radius and H is the altitude of the cube-sat. Both EAD and T_{orbit} are functions of the altitude H which is an uncertain parameter. For each completed orbit the amount of images generated is:

$$\mathbf{N}_{pic}(FR, H) = [N_1, N_2, \dots, N_o] \quad (19)$$

where N_o is the number of pictures in the last completed orbit and FR is the frame rate - function of H and bounded by the FR_{max} . The corresponding amount of data generated in the Payload System in all the orbits is accounted in the vector \mathbf{V}_{PL} :

$$\mathbf{V}_{PL} = \frac{IS \cdot BD \cdot \mathbf{N}_{pic}}{8 \cdot 2^{30}} \quad (20)$$

where IS (image size) and BD (bit depth) depends on the type of payload and the denominator change units from bits to Giga bytes.

Data is compressed and accumulated in the OBDH System and sent to the ground station when the cubesat is in view. The coverage area of the satellite is a circular area on the Earth surface in which the satellite can be seen under an elevation angle ϵ

$$S_{coverage} = 2\pi R_E^2 (1 - \cos \zeta) \quad (21)$$

with ζ the earth central angle that can be evaluated from:

$$\epsilon + \eta + \beta = 90 \quad (22)$$

$$d \cdot \cos \epsilon = r \cdot \sin \zeta \quad (23)$$

$$d \cdot \sin \eta = R_e \cdot \sin \zeta \quad (24)$$

where ϵ is the elevation angle, η the nadir angle, β the central angle, d the distance between ground station and cube-sat, R_e the distance between the ground station and the Earth centre and $r = R_e + H$ where H is the altitude. The biggest area correspond to $\epsilon = 0$ but it can be affected by some natural barriers or general obstacles, then the minimum acceptable ϵ_{min} is modelled as an uncertain angle > 0 . The total time in view, the access time T_{ac} , is:

$$T_{ac} = \frac{T_{orbit}}{180^\circ} \arccos \frac{\cos(\zeta_{max})}{\cos(\zeta_{min})} \quad (25)$$

where

$$\zeta_{max} = 90^\circ - \epsilon_{min} - \eta_{max} \quad (26)$$

$$\sin(\eta_{max}) = \sin \frac{EAD}{2} \cos \epsilon_{min} \quad (27)$$

$$\sin(\zeta_{min}) = \sin(lat_{pole}) \sin(lat_{GS}) + \quad (28)$$

$$\cos(lat_{pole}) \cos(lat_{GS}) \cos(\Delta long) \quad (29)$$

with ϵ the elevation angle, η the nadir angle, $lat_{pole} = 90^\circ - I$ with I the inclination, lat_{GS} the latitude of the ground station and $\Delta long$ the difference in longitude between orbit pole and ground station [10].

Access Time and Data Volume are time dependent: $T_{ac}(t)$ and $DV(t) \forall t \in [T_0, T_{Mission}]$. Finally, some of the

outputs - the amount of uncompressed data DV , the access time T_{ac} , the required power $P_{payload}$ and the momentum of inertia I_z - are inputs for other nodes in the network, as it is explained by Figure 1.

5.3 On board data handling (OBDH)

Ground station can communicate with the LEO satellite only when it is in the visibility region; since is not affordable to sent all the data accumulated during each orbit to the ground station during this small fraction of time, OBDH system is needed to compress the images arriving from the payload and store them. JPEG compression is used to obtain V_c and high quality (10:1) for land pictures while medium quality (20:1) for water areas. Mass M_{OBDH} and power P_{OBDH} are evaluated as function of uncompressed data V and the access time T_{ac} .

The amount of data after the compression, for each orbit, is evaluated from Equation 20:

$$\mathbf{V}^c = [V_1^c, V_2^c, \dots, V_i^c, \dots, V_o^c] \leftarrow \mathbf{V}_{PL} \quad (30)$$

where V_o^c is the compressed amount of data of the last orbit N_o and all the V_i^c are considered in order to evaluate the performance indicator in Equation 15.

5.4 Telecommunication (TTC)

Telecommunication subsystem, composed of an antenna (ant), an amplified transponder (amp) and a radio frequency distribution network (rfdn), connects the transmitter antenna on the cube-sat with the receiving antenna on the ground station.

First the type of antenna is chosen with regard to the transmitter antenna gain G_t : patch antenna when $5 \leq G_t < 10$, horn antenna when $10 \leq G_t < 20$ and parabolic antenna when $G_t \geq 20$. Evaluated the diameter D and half-power beam-width θ as:

$$D = \frac{wl}{\pi} \sqrt{\frac{G_t}{\eta_{ant}}} \quad (31)$$

$$\theta = 41253 \frac{\eta_{ant}}{G_t} \quad (32)$$

with η_{ant} the antenna efficiency and wl the wave length, mass is calculated for the chosen antenna type. For patch antenna:

$$M_{ant} = \pi \frac{D^2}{4} (0.0005\rho_c + 0.0015\rho_d) \quad (33)$$

with ρ_c and ρ_d respectively density of copper and density of dielectric material. For a horn antenna:

$$M_{ant} = S_{horn} \cdot \rho_{horn} \quad (34)$$

with S_{horn} the lateral surface of the conic horn and ρ_{horn} the surface density. For a parabolic antenna:

$$M_{ant} = 2.89D^2 + 6.11D - 2.59 \quad (35)$$

where the formula can be found in [11].

Mass of M_{rfdn} is given as input while mass M_{amp} , as well as power requirement P_{amp} , for the amplified transponder are derived from available data as described in [12], as function of the transmitter power P_t (power in output from the antenna).

$$P_t = \frac{E_b}{N_0} - G_t - L_t - L_s - L_p - \frac{G_r}{T_s} + 10 \cdot \log_{10} R - 228.6 \quad (36)$$

where $\frac{E_b}{N_0}$ is the ratio of received energy-per-bit to noise density, L_t is the on board loss, L_s is the free space path loss, L_p is the propagation loss, G_r the receiver antenna gain, T_s the system noise temperature and $R = \frac{V}{T_{ac}}$ the data rate where V (bits) is the transmitted data and T_{ac} the access time (seconds) to the ground station.

Finally, the mass of the TTC is the sum of the components:

$$M_{TTC} = M_{ant} + M_{amp} + M_{rfdn} \quad (37)$$

and the power is function of the transponder only:

$$P_{TTC} = P_{amp} \quad (38)$$

5.5 Attitude and orbit control (AOC)

Attitude and orbit control system is in charge to control the position and the orientation of the cubesat with a three axis stabilisation; the actuators used are reaction wheels (RW) and magneto-torques (MT).

During the mission, the cube-sat is affected by some disturbances, in particular the solar pressure T_s , the magnetic torque T_m , the aerodynamic drag T_a and the gravity gradient torque T_g .

$$T_s = \frac{I_s}{c} Al(1 + q) \quad (39)$$

with I_s the incident solar array, c the speed of light, A the area of the cube-sat normal to the Sun, l the offset between the centre of gravity and centre of pressure of the satellite and q the reflectance factor.

$$T_m = m \frac{B_0 R_e^3}{(R_e + h)^3} \sqrt{3 \sin^2(lat) + 1} = mB \quad (40)$$

where m is the spacecraft residual dipole, B_0 is the planets magnetic field strength, R_e is the planet radius, h is the altitude, lat is the magnetic latitude.

$$T_a = \frac{1}{2} \rho v^2 C_D Al \quad (41)$$

where ρ is the atmospheric density at the spacecraft altitude, v is the spacecraft velocity, C_D is the drag coefficient of the spacecraft, A is the area of the spacecraft normal to the velocity vector.

$$T_g = \frac{3\mu}{2(R_e + h)^3} |I_z - \min(I_x, I_y)| \sin 2\psi \quad (42)$$

where μ is the planet gravitational parameter, I_z is the maximum moment of inertia of the satellite, and ψ is the angle between the spacecraft z axis and the nadir vector.

The total disturbance is the sum:

$$T_d = T_s + T_m + T_a + T_g \quad (43)$$

The momentum stored due to the disturbance in the RW, H_d , the momentum required for the slew manoeuvres H_{slew} and the detumbling manoeuvre H_{det} are:

$$H_d = \frac{T_d P}{4e} \quad (44)$$

$$H_{slew} = T_{slew} \cdot t_{slew} \quad (45)$$

$$H_{tumbl} = I_z \cdot spin_{rate} \quad (46)$$

with P the orbital period, e the pointing accuracy, T_{slew} , t_{slew} , I_z and $spin_{rate}$.

Mass, M_{rw} , and power, P_{rw} , for the RW are computing by interpolation from available real data, in function of the maximum between H_d , H_{slew} and H_{tumbl} :

$$M_{rw} \propto \max(H_d, H_{slew}, H_{tumbl}) \quad (47)$$

$$P_{rw} \propto \max(H_d, H_{slew}, H_{tumbl}) \quad (48)$$

To unload momentum stored in the RW, mass and power of MT are interpolated in function of the required magnetic dipole D_{mag} :

$$M_{MT} \propto D_{mag} \quad (49)$$

$$P_{MT} \propto D_{mag} \quad (50)$$

where

$$D_{mag} = \frac{T_d}{B} \quad (51)$$

with B given in Equation 40.

Finally, the outputs of the AOCS node are:

$$M_{AOCS} = M_{rw} + M_{MT} \quad (52)$$

$$P_{AOCS} = P_{rw} + P_{mt} \quad (53)$$

5.6 Power

The electrical power system (EPS) is composed of a solar array, a battery pack, a power conditioning and distribution

unit (PCDU). The mass of the power system is the sum of the individual masses of the components

$$M_{power} = M_{SA} + M_{BP} + M_{PCDU} \quad (54)$$

The power produced by the system is the power converted by the solar array

$$P_{power} = P_{sa} \quad (55)$$

Given the power requirement P_n for the spacecraft night, as well as the duration t_n of the night, the energy capacity requirement of the battery system is

$$E_{req} = \frac{P_n t_n}{\eta_{b-l} DOD} \quad (56)$$

where η_{b-l} is the transfer efficiency between battery and loads, and is the product of the efficiencies of the battery discharge regulator, the distribution unit, and the harness:

$$\eta_{b-l} = \eta_{bdr} \eta_{distr} \eta_{harn} \quad (57)$$

The efficiency η_{bdr} of the battery discharge regulator is a function of the bus voltage, and can assume values between 0.9 at 20 V and 0.97 at 100 V. In case of unregulated bus, η_{bdr} , as there is no discharge regulator. The harness efficiency η_{harn} is

$$\eta_{harn} = 1 - \frac{V_{drop}}{100} \quad (58)$$

and is therefore dependent on the allowable voltage drop V_{drop} given as a percentage of the bus voltage. The efficiency of the distribution unit is $\eta_{distr} = 0.99$. The depth of discharge DOD is function of the number CL of charge/discharge cycles, that is dependent on the mission time. Their relationship is estimated as [9]

$$DOD(t) = -36.76 \ln \frac{CL(t)}{207800} \quad (59)$$

Given the energy requirement for the battery, the mass of the battery pack is

$$M_{batt} = \frac{E_{req}}{E_{cell}} \quad (60)$$

where E_{cell} is the energy density (Wh/kg) of the cell, given in input. Finally, the charging efficiency η_{batt} of the battery is computed by interpolation of efficiencies [0.82, 0.83, 0.835, 0.95] and energy densities [37, 44, 51, 135] Wh/kg. The power P_{sa} required from the solar array is computed from the power requirements P_d and P_n for the spacecraft daylight and night periods respectively, as well as the durations t_d and t_n of the periods

$$P_{sa} = \frac{P_n t_n}{\eta_{a-b} \eta_{b-l} t_d} + \frac{P_d}{\eta_{a-l}} \quad (61)$$

where η_{a-b} is the transfer efficiency between solar array and battery pack, η_{a-l} is the transfer efficiency between solar array and loads. The power requirements are a typical epistemic uncertainty in preliminary design, therefore an uncertainty factor δP is applied to P_d and P_n . The transfer efficiencies can be expressed as the product of the efficiencies of the components:

$$\eta_{a-b} = \eta_{sar} \eta_{bcr} \eta_{batt} \quad (62)$$

$$\eta_{a-l} = \eta_{sar} \eta_{distr} \eta_{harn} \quad (63)$$

where η_{bcr} is the efficiency of the battery charge regulator and, as for the discharge regulator, can assume values between 0.9 at 20 V and 0.97 at 100 V, or 1 if the bus is unregulated, and η_{sar} is the efficiency of the solar array regulator, and assumes values between 0.94 at 20 V and 0.99 at 100 V for direct energy transfer (DET) configuration, or between 0.93 at 20 V and 0.97 at 100 V for maximum power peak tracking (MPPT) configuration. Solar cells suffer from several factors that decrease their efficiency. Increasing the temperature of the cell reduces the power generated by the cell. At a certain temperature T , the change in efficiency is given by

$$\eta_{temp} = 1 - \eta_T (T - T_{nom}) \quad (64)$$

where η_T is the degradation per centigrade, which assumes values between 0.005 for cell efficiency of 0.16, and 0.002 for cell efficiency of 0.28, and T_{nom} is the nominal temperature of the solar cell, usually 28 °C. Several other factors concur at degrading the efficiency of the solar cell. The array pointing loss factor is

$$\eta_p = \cos \alpha \quad (65)$$

where α is the solar incidence angle. The distance r_S (in AU) from the Sun involves a loss, or gain, that is

$$\eta_r = \frac{1}{r_S^2} \quad (66)$$

Furthermore, cells degrade with time mainly due to radiation fluence, and such degradation can be estimated as in [8]

$$\eta_{life}(t) = (1 - D_{cell})^t \quad (67)$$

where D_{cell} is the cell degradation per year, and $T_{Mission}$ is the cell life time (the mission time). A further important factor affecting the efficiency of the solar array is the assembly efficiency η_a . The efficiency of the array is lower than the efficiency of the single cells because of a loss due to assembly. Such factor is usually uncertain and is given as input. The total cell efficiency is therefore

$\eta_{tot} = \eta_a \eta_{temp} \eta_p \eta_r \eta_{life}$. The specific power (Wh/m²) of the array is

$$P_{cell} = 1370 \eta_{cell} \eta_{tot} \quad (68)$$

From this, the required area of the array is computed

$$A_{sa} = \frac{P_{sa}}{P_{cell}} \quad (69)$$

and finally the mass of the solar array

$$M_{sa} = A_{sa} \rho_{sa} \quad (70)$$

The PCDU is a modular unit composed of modules such as battery charge and discharge regulators, solar array regulators, maximum power point tracker, shunt regulator, distribution unit (latching current limiters), telemetry interface. The number of modules, and therefore the mass of the unit, is dependent on the power system configuration. Indeed, if the bus is unregulated, there are no battery charge and discharge regulators, therefore the PCDU is lighter. If the configuration is DET, there is no maximum power point tracker, and the PCDU is lighter. On the other hand, an MPPT configuration extract maximum power from the solar array, therefore the array size decreases, but the presence of the MPPT module decreases the transfer efficiency and increases the PCDU mass. The configuration is a typical trade-off in the design, and is a design parameter. The mass M_{pcdu} can be estimated as the sum

$$M_{pcdu} \mu_{pcdu} (2P_{sa} + bP_d + bP_e + cP_{sa}) \quad (71)$$

where $\mu_{pcdu} = 0.001$ kg/W, b is the bus type (0 for unregulated, 1 for regulated bus), c is the configuration (0 for DET, 1 for MPPT), and the 2 multiplying the first term in brackets accounts for a telemetry and a distribution unit.

6. Dynamic multi-state systems

In this section, we will describe, how we include possible satellite failure modes into our performance calculations. A system is called multi-state when it can have multiple states and the number of possible states are finite. The set of all the possible states is denoted by \mathcal{X} . A stochastic process is a collection of random variables $\{X(t)\}_{t \in \mathcal{T}}$ representing the system state in time and its dynamics can be generally described by a family of transition operators $T_s^t : \mathcal{X} \times \mathcal{X} \rightarrow [0, 1]$, so that $T_s^t(x, y)$ models the probability that the system is in state y at time t given that it was in state x at time s . By applying a sequence of transition operators the law of the state of the satellite at any time t can be derived given the law at time for $X(0)$.

This stochastic dynamics above is continuous in time; however, the data acquisition procedure explained in the Section 5.2 is discontinuous. Therefore in our model, the data which was acquired during a complete orbit cycle was distributed uniformly through the entire cycle to model the *instantaneous data increment* at any time. This assumption makes it possible to handle the data volume as a continuous variable in time and hence to calculate its expected value with regard to the stochastic evolution of the system state. In a given time t , the instantaneous data increment is denoted as $V(t; d, u)$. The expression for the performance measure of the accumulated data dependent on the satellite will thus take the following form:

$$f_{DV}(\mathbf{d}, \mathbf{u}) := \mathbb{E} \left\{ \int_0^{T_{Mission}} V(t, X, \mathbf{d}, \mathbf{u}) dt \right\} \quad (72)$$

If the evolution of the stochastic process (transition operator T) is not dependent on V , the integration over time can be taken out from the expected value calculation by applying the Fubini theorem [13]. Furthermore, if the instantaneous data increment V depends only on the current state and not on the state history, the expression for computation of the expected data gain will take the following form:

$$f_{DV}(\mathbf{d}, \mathbf{u}) := \int_0^{T_{Mission}} \mathbb{E} \{V(t, X(t), \mathbf{d}, \mathbf{u})\} dt, \quad (73)$$

where $X(t)$ is a random variable modelling the state of the system at time t .

After the transition operator of the satellite state and the instantaneous data increments are defined for each states $X(t) = x_i$ (where $i = 1..N$) the Equation (73) express the stochastic law of the accumulated data during the mission of the satellite.

6.1 Reliability and resilience

Two directions of the system state transition are considered. The fully or partially functional system can deteriorate or the partially functional system can recover. Once a total failure of the system occurred the system is not able to recover anymore and the satellite is considered lost. The time dependent reliability of a satellite is typically modelled by a Weibull distribution [14, 15]. This work also adopts the Weibull distributions for modelling the reliability, the transition between both functional states to the failure state. The system can be in 3 states. State 0: total system failure (x_0); state 1: partially functional system (x_1) or state 2: fully functional system (x_2). The satellite is assumed to be fully

functional at the start of its operations ($X(0) = x_2$). The probability that a system failure occurs at time T_{fail} have a Weibull distribution regardless if the system was in x_2 or x_1 . Before the T_{fail} , a simple alternation process is used to model the transition between states x_1 and x_2 by a time-homogeneous continuous time Markov Chain. This models the occurrence of less severe failures and their repair, by which we model the reconfiguration of the system. The stochastic dynamics of this alternation process are given by the following transition operator:

$$T_s^t(x, y) = \exp\{Q(t - s)\}(x, y), \quad (74)$$

such that the transition rate Q (an analogue to the time derivative for ordinary differential equations) is dependent on the design and uncertain parameters,

$$Q(\mathbf{d}, \mathbf{u}) = \begin{pmatrix} -\mu(\mathbf{d}, \mathbf{u}) & \mu(\mathbf{d}, \mathbf{u}) \\ \lambda(\mathbf{d}, \mathbf{u}) & -\lambda(\mathbf{d}, \mathbf{u}) \end{pmatrix}, \quad (75)$$

where the first line and column refer to state x_1 and the second ones to state x_2 , and μ and λ are some functions of both design and uncertain parameters. The state changes from x_2 to x_1 with rate λ and with rate μ in the opposite way.

The probability that the system is in state x_0 is given by the cumulative distribution function of the Weibull distribution and is denoted by $p_0(t)$.

The probability of that the system is in state x_2 given the system is in state x_1 or x_2 (i.e. that the fatal failure has not occurred yet) is:

$$\begin{aligned} \Pr(X(t) = x_2 | X(t) \in \{x_1, x_2\}, X(0) = x_2) = \\ = \frac{\mu}{\mu + \lambda} + \frac{\lambda}{\mu + \lambda} \exp(-t(\mu + \lambda)) =: p_2(t). \end{aligned} \quad (76)$$

Respectively, the probability of that the system is in state x_1 given that the system has not been lost is $p_1(t) = 1 - p_2(t)$.

Therefore, the expected value of the instantaneous data increment is expressed as:

$$\begin{aligned} \mathbb{E}\{V(t, X(T)\mathbf{d}, \mathbf{u})\} = \\ [V_2(t; \mathbf{d}, \mathbf{u})p_2(t) + V_1(t; \mathbf{d}, \mathbf{u})p_1(t)](1 - p_0(t)) + \\ + V_0(t; \mathbf{d}, \mathbf{u})p_0(t), \end{aligned} \quad (77)$$

where V_i represents the instantaneous data increment in the respective state x_i .

The instantaneous $V_2(t)$ - totally functioning state - can be approximated from Equation 30 by interpolation in time:

$$V_2(t) \leftarrow \mathbf{V}^c \quad (78)$$

while $V_1(t)$ - partially functioning state - we will model in this example as a function of $V_2(t)$:

$$V_1(t) = \frac{V_2(t)}{2} \quad (79)$$

and $V_0(t)$ - the state of total failure - represents generation (or transmission) of no additional data:

$$V_0(t) = 0. \quad (80)$$

6.2 Used probability distributions

Disclaimer: The dependency between the design and uncertainty parameters and the parameters of the probability laws governing the stochastic evolution of the system state have both been chosen artificially for the purposes of our experiments in order to derive and test the methodology. We choose not to include the actual parameters used in our computation in order not to mislead anyone. The proper influence of the parameters will be investigated in the future work. In the rest of the section, we will only briefly elaborate on how the laws of the stochastic process were composed.

The parameters of the distribution governing the total failure law of the satellite is based on the coefficients for satellite subsystem failure rate inferred in [15]. The probability of satellite survival, $1 - p_0(t)$, is calculated as the probability that all the subsystems have survived, i.e. a product of their respective survival functions.

The parameters of the alternating process were “elicited” in the following way. Parameter μ remains fixed on the value $1/365$. For the parameter λ , first, we have chosen its base value to be $\lambda_0 = 1/365$. Then, each of the design and uncertain parameters were assessed, whether it could, by our guess, influence the partial failure rate λ , and the extreme values of the relative influence. For each parameter, the relative influence, say $r_{u,i}(u_i)$ and $r_{d,i}(d_i)$, where u_i and d_i represent elements of the design and uncertainty parameter vectors, was calculated by an interpolation between these extreme values. The final value of the partial failure rate is then calculated as:

$$\lambda(\mathbf{d}, \mathbf{u}) = \lambda_0 \cdot \prod_i [r_{u,i}(u_i)] \prod_i [r_{d,i}(d_i)].$$

7. Results

Figure 2 presents the solution of Problem 16 that is the MO min-max approach: it is a Pareto front between the two

conflicting objectives Mass and Expected value of the cumulative Data Volume. The red point in the Pareto front, instead, corresponds to the solution of the Single objective minmax.

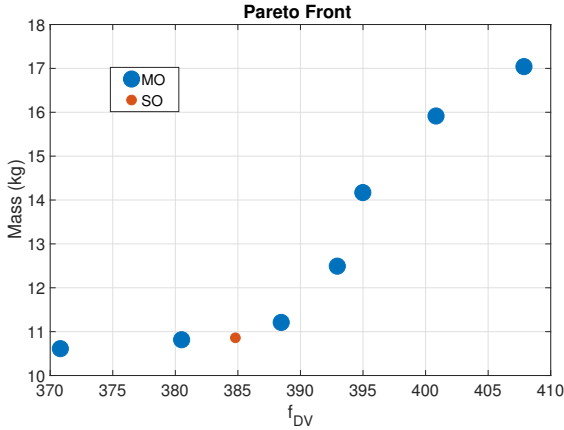


Fig. 2: Comparison between Single Objective approach and Multi Objective approach: the red point has been evaluated with a weighted function between mass and Data Volume.

Solution of problem 17 is, instead:

$$\min_{\mathbf{d} \in D} \max_{\mathbf{u} \in U} \frac{M_{TOT}(\mathbf{d}, \mathbf{u}, t)}{f_{DV}(\mathbf{d}, \mathbf{u}, t)} = 0.028 \quad (81)$$

and the parameters $[\mathbf{d}, \mathbf{u}]_{minmax}$ correspond to:

- Mass= 10.86 kg
- DV = 384.8 GB

The SO solution is added to the Pareto front of figure 2 and refers to a decision for which objective functions have similar weights.

From this solution the Belief surface has been calculated and plotted in Figure 3 and 4. The 3D Belief has been evaluated from Equation 5 with:

$$A = \{\mathbf{u} \in U \mid Mass(\mathbf{d}, \mathbf{u}, t) \leq \nu \wedge f_{DV}(\mathbf{d}, \mathbf{u}, t) \geq \mu\}. \quad (82)$$

Finally, Figure 5 shows also a comparison with the classical approach of margins. For both the quantities of interest, the optimal solution in the design space has been evaluated with the nominal values of the uncertainty parameters (green point). The solution with margins corresponds to the blue point in figure, where 20% of margin has been applied to all the quantities that are exchanged between the nodes of the network in Figure 1 and finally to the quantities of interest.

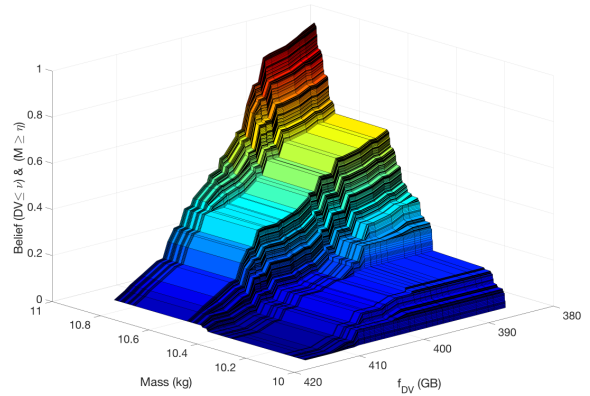


Fig. 3: bi-objective belief. The surface show the lower bound of the probability (the belief) that the two objective functions are below (mass) or above (f_{DV}) two given thresholds.

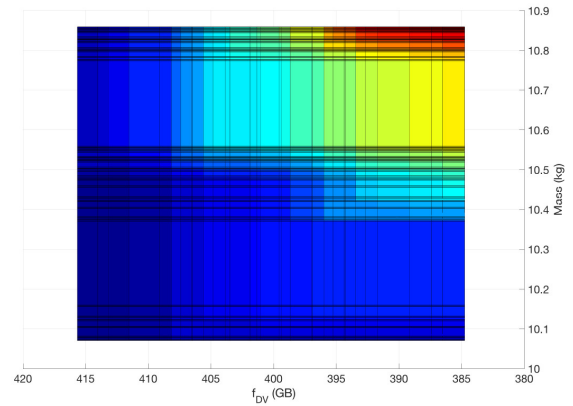


Fig. 4: bi-objective belief. This plot shows the same results as Figure 3, from a different point of view; cold colours correspond to low belief values while warm colours to high belief values.

8. Conclusions

A method for robust optimisation under the presence of severe uncertainty has been presented. Due to the complexity of calculations with uncertainty described by the DST, the optimisation was formulated to minimise the constrained worst case scenario, with constraint being the reliability of the satellite during its mission, which was effectively solved by a memetic algorithm for constrained min-max optimisation described in Section 4. Once the solution was obtained, it was consequently subjected to an uncer-

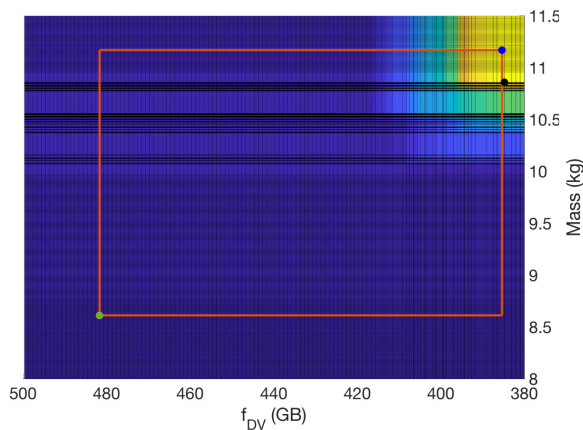


Fig. 5: Colours from blue to yellow represent the value of belief (from zero to one). The green dot corresponds to the nominal solution, the blue one to the nominal solution with margins and the black dot to the worst case scenario.

tainty analysis according to the DST and the corresponding Belief in the values of the performance of the optimised design was reconstructed according to the approximation algorithm described in Section 3.

The resilience, the system responsibility to random failures, has been added into the model specification by considering possible reconfiguration of the system functionality after a partial failure. This has been modelled by a simple homogeneous Markov Chain described in Section 6. Although, the authors are aware, that the used model does not properly reflect the actual dynamics of the system, not only because of the usage of artificial dependencies of the parameters governing the stochastic evolution on the design and uncertainty parameters, but also because of usage of a the Markov process and omitting the influence of possible loss of performance after the reconfiguration of the system. These simplifications were made mainly in order to simplify the derivation of the framework of expected performance optimisation which better reflects the uncertainties about the performance of a system in uncertain conditions and will be addressed in more detail in the future work.

Acknowledgement

The work in this paper was supported by the H2020-MSCA-ITN-2016 UTOPIAE, grant agreement 722734.

References

- [1] M. Vasile. “On the Solution of Min-Max Problems in Robust Optimisation”. In: *The EVOLVE*. 2014.

- [2] M. Di Carlo, M. Vasile, and E. Minisci. “Multi-population inflationary differential evolution algorithm with Adaptive Local Restart”. In: *IEEE Congress on Evolutionary Computation (CEC)*. 2015.
- [3] G. Filippi et al. “Evidence-Based Robust Optimisation of Space Systems with Evidence Network Models”. In: *IAAA CEC 2018*, 2018.
- [4] J. C. Helton. “Uncertainty and sensitivity analysis in the presence of stochastic and subjective uncertainty”. In: *Journal of Statistical Computation and Simulation* 57 (1997), pp. 3–76.
- [5] W.L. Oberkampf and J.C. Helton. “Investigation of Evidence Theory for Engineering Applications”. In: *AIAA 2002-1569, Denver Colorado*. 4th Non-Deterministic Approaches Forum. 2002.
- [6] G. Shafer. *A mathematical theory of evidence*. Princeton University Press, 1976.
- [7] M. Vasile and S. Alicino. “Evidence-based preliminary design of spacecraft”. In: *SECESA 2014*, 2014.
- [8] M. Vasile et al. “Fast Belief Estimation in Evidence Network Models”. In: *EUROGEN 2017*. 2017.
- [9] G. Filippi et al. “Evidence-Based Robust Optimisation of Space Systems with Evidence Network Models”. In: *SECESA 2018*, 2018.
- [10] G.D. Gordon and W.L. Morgan. *Principles of communication satellites*. John Wiley and sons, Inc., 1993.
- [11] C.D. Brown. *Elements of Spacecraft Design*. AIAA Education Series, 2002.
- [12] J.R. Wertz and W.J. Larson. *Space Mission Analysis and Design*. 3rd ed., Microcosm Press, 1999.
- [13] G. Fubini. “Sugli integrali multipli”. In: *Rend. Acc. Naz. Lincei*. 1907, pp. 608–614.
- [14] J.F. Castet and J.H. Saleh. “Satellite and satellite subsystems reliability: Statistical data analysis and modeling”. In: *Reliability Engineering and System Safety* 94(11), (2009), pp. 1718–1728.
- [15] J.F. Castet and J.H. Saleh. “Beyond reliability, multi-state failure analysis of satellite subsystems: a statistical approach”. In: *Reliability Engineering and System Safety* 95(4) (2010), pp. 311–322.